

Intra- and Inter-chain Fluctuations in Entangled Polymer Melts in Bulk and Confined to Pore Channels

Rainer Kimmich¹, Nail Fatkullin², Ralf-Oliver Seitter¹, Elmar Fischer¹,
Uwe Beginn³, Martin Möller³

¹Universität Ulm, Sektion Kernresonanzspektroskopie, 89069 Ulm, Germany

²Kazan State University, Department of Molecular Physics, 420008 Kazan,
Russia/Tatarstan

³Universität Ulm, Abteilung Makromolekulare Chemie, 89069 Ulm, Germany

SUMMARY: It is known that topological restraints by “chain entanglements” severely affect chain dynamics in polymer melts. In this field-cycling NMR relaxometry and fringe-field NMR diffusometry study, melts of linear polymers in bulk and confined to pores in a solid matrix are compared. The diameter of the pore channels was 10 nm. It is shown that the dynamics of chains in bulk dramatically deviate from those observed under pore constraints. In the latter case, one of the most indicative signatures of the reptation model is verified 28 years after its prediction by de Gennes: The frequency and molecular mass dependencies of the spin-lattice relaxation time obey the power law $T_1 \propto M^0 \nu^{3/4}$ on a time scale shorter than the longest Rouse relaxation time τ_R . The mean squared segment displacement in the pores was also found to be compatible to the reptation law $\langle r^2 \rangle \propto M^{-1/2} t^{1/2}$ predicted for $\tau_R < t < \tau_d$, where τ_d is the so-called disengagement time. Contrary to these findings, bulk melts of entangled polymers show frequency and molecular mass dependencies significantly different from what one expects on the basis of the reptation model. The data can however be described with the aid of the renormalized Rouse theory.

Introduction

In his famous 1971 paper, de Gennes¹⁾ treated what he termed “*Reptation of a polymer chain in the presence of fixed obstacles*”. The spin-lattice relaxation time T_1 was predicted to follow the power law

$$T_1 \propto M^0 \nu^{3/4} \quad \text{for } \tau_e < t < \tau_R, \quad (1)$$

where τ_R is the longest Rouse relaxation time and τ_e is the so-called entanglement time. Another prediction of the reptation model²⁾ is that the mean squared segment displacement obeys

$$\langle r^2 \rangle \propto M^{-1/2} t^{1/2} \quad \text{for } \tau_R < t < \tau_d, \quad (2)$$

where τ_d is the tube disengagement time. The complete set of limiting laws for spin-lattice relaxation and the mean squared segment displacement expected on the basis of the tube/relaxation model is summarized in Tab. 1.

The tube/reptation concept²⁾ is widely considered for the description of “entangled dynamics” in polymer fluids with chain lengths above the critical value. However, despite many attempts, the combined frequency dispersion and (absent) molecular mass dependence given at Eq. (1) was never found in melts of entangled polymers^{3,4)}. Also, the molecular weight dependence of the mean squared segment displacement expected according to Eq. (2) did not show up^{5,6)}, and curve fitting attempts led to unrealistic parameter values⁷⁾.

The situation becomes very different if the polymer chains are confined to artificial “tubes” in the form of the pores of nanoporous media. In the present paper, we report on the first experimental verification of the law given in Eq. (1). Also, reasonable agreement with Eq. (2) was found. Polymer chain dynamics have been studied using fringe-field NMR diffusometry and proton and deuteron field-cycling NMR relaxometry⁸⁾. With the latter technique, the accessible frequency range is 100 Hz to 100 MHz. Fringe-field NMR diffusometry permits one to study translational segment diffusion on a time scale reaching down to less than 100 μ s. Both methods taken together thus are suitable to probe chain modes of entangled polymers. Using these techniques the effect of artificial topological restraints on polymer dynamics was studied^{9,10)} by incorporating flexible linear polymer chains in a porous medium in order to have “obstacles” in the form of pore walls in analogy to de Gennes’ model.

Table 1. Limits for translational segment diffusion and spin-lattice relaxation predicted by the tube/reptation model. (t , time; ω , angular Larmor frequency; M , molecular mass; τ_s , Kuhn segment fluctuation time; α , unspecified exponent in the range 1 ... 2)

	limit	mean squared segment displacement	spin-lattice relaxation time
I	$\tau_s \ll (t, 1/\omega) \ll \tau_e$	$\langle r^2 \rangle \propto M^0 t^{1/2}$	$T_1 \propto -M^0 / \ln(\omega \tau_s)$
II	$\tau_e \ll (t, 1/\omega) \ll \tau_R$	$\langle r^2 \rangle \propto M^0 t^{1/4}$	$T_1 \propto M^0 \omega^{3/4}$
III	$\tau_R \ll (t, 1/\omega) \ll \tau_d$	$\langle r^2 \rangle \propto M^{-1/2} t^{1/2}$	$T_1 \propto M^{-1/2} \omega^{1/2}$
IV	$\tau_d \ll (t, 1/\omega)$	$\langle r^2 \rangle \propto M^{-2} t^1$	$T_1 \propto M^{-\alpha} \omega^0$

There is a number of earlier attempts to study confinement effects of organic polymers filled into nanoporous silica glasses¹¹⁻¹⁷⁾. However, the interpretation in this case is difficult because adsorption and geometrical restriction effects must be distinguished. Ideally, one would like to study free linear polymers in immobilized networks formed of the same polymer species. As this is experimentally not feasible, we have mimicked the “tube” by semi-interpenetrating networks. That is, linear polymers are confined in a matrix also of an organic polymer nature.

The bi-continuous semi-interpenetrating networks studied in this work are much less prone to the influence of adsorption on the dynamics of the incorporated linear polymers. Furthermore, no problem arises in imbibing the porous medium with the polymers of interest, because the samples are prepared in a way that the diffusing species are a priori dispersed in the host material.

Samples and Techniques

Linear perdeuterated polyethyleneoxide (PEO-d4) was studied in the pore channels in a matrix of cross-linked polyhydroxyethylmethacrylate (PHEMA) with radii in the order of 5 nm. The preparation and characterization of these semi-interpenetrating networks by various non-NMR methods are described in Ref. 9. The PEO bulk root mean square chain end-to-end distances partly exceeded the mean pore radius significantly. The neutron scattering value of the molecular-weight related mean square chain end-to-end distance, i.e. R^2 / M_w , where R is the root mean squared chain end-to-end distance, is about^{18,19)} $1 \times 10^{-20} \text{ m}^2 \text{ mol/g}$ in bulk PEO melts at 80 °C. On this basis, the root mean squared chain end-to-end distances under unperturbed conditions is estimated as 8.6, 13.2, and 20.9 nm for our PEO samples with M_w equal to 7400, 17300, and 43200, respectively.

The PHEMA matrix was strongly cross-linked, that is, in the average, cross-links occur every six monomers. DSC thermograms appear to indicate a glass transition at about 68 °C, but the change in the specific heat is extremely weak. Anyway, the molecular mobility in the matrix at the temperature of the present experiments (80 °C) can be considered to be strongly suppressed. Even at 100 °C, i.e. 20 °C above the measuring temperature, the macroscopic hardness is comparable to that in the true glassy state.

The deuteron spin-lattice relaxation dispersion, $T_1 = T_1(\nu)$, of perdeuterated PEO in the undeuterated PHEMA matrix as well as in bulk was examined mainly with the aid of deuteron field-cycling NMR relaxometry⁸⁾. Choosing deuteron resonance ensured that the spin-lattice relaxation of PEO was selectively measured, and that no spin exchange processes with the undeuterated PHEMA matrix mattered.

The home built field-cycling relaxometer is specified in detail in Ref. 20. The detection magnetic flux density was 1.5 T, the reproducibility in subsequent field cycles and stability better than 10^{-5} . All spin-lattice relaxation curves were monoexponential over at least a

decade. The transverse relaxation curves measured with a conventional 9.4 T NMR spectrometer were approached by exponential decays with insignificant deviations.

Characteristic Time Constants of the Tube Model for PEO

The dynamic limits of the tube/reptation model are defined by a series of characteristic time constants. The tube disengagement time can be expressed as²⁾

$$\tau_d = \frac{R^2}{3\pi^2 D} \quad , \quad (3)$$

where D is the center-of-mass diffusion coefficient. Note that τ_d is a parameter derived under the assumption that the lengths of the tube and of the primitive path coincide. However, in the PHEMA matrix, the “tube” is determined by the pore structure⁹⁾ rather than by the linear PEO chains incorporated in the pores. This parameter is therefore not only determined by the chain length, but also by the distance of nearest branching points of the pores. Thus, the disengagement time in pores must be expected to be much longer than in unconfined melts.

The (longest) Rouse relaxation time is related to the tube disengagement time (under the conditions originally anticipated) by

$$\tau_R = \frac{M_c}{6M_w} \tau_d \quad , \quad (4)$$

where M_w and M_c are the weight average molecular mass and the critical molecular mass, respectively. The third time constant of interest here, namely the entanglement time, τ_e , can be estimated as the Rouse relaxation time for $M_w = M_c / 2$. Finally, the segment fluctuation time, τ_e , can be directly be read out from the T_1 minimum (see Ref. 4).

For PEO, we have $M_c = 3600$ and^{18,19)} $R^2 / M_w \approx 1 \times 10^{-20} \text{ m}^2$. The center-of-mass diffusion coefficient can be calculated for each chain length based on the experimental reference value $D_{ref} = 3 \times 10^{-13} \text{ m}^2/\text{s}$ which holds for $M_{ref} = 12\,300$ (after correction for the different temperature of our samples, 80 °C)^{9,21,22)} according to

$$D = \left(\frac{M_{ref}}{M_w} \right)^2 D_{ref} \quad , \quad (5)$$

where the known square molecular-mass dependence of the center-of-mass diffusion coefficient was taken into account.

Based on these data and referring to the original definitions for bulk systems, we estimate the Rouse and disengagement times listed in Tab. 2 for the molecular masses of our samples. The (chain length independent) entanglement time is estimated to be of the order 10^{-8} s. From the temperature/frequency position of the T_1 minimum, the segment fluctuation time is expected to be less than 10^{-9} s at 80 °C. As the frequency scale of this study is limited by $\nu \leq 6 \times 10^7$ Hz, any significant influence of limit I on our data can be excluded. On the other hand, the frequency ranges, where limits III and IV could play a role in principle, are limited by $\nu < \nu_R$ and $\nu < \nu_d$, where the ν_R and ν_d values relevant for our samples are given in Tab. 2.

Table 2. Time constants of the tube model semi-empirically estimated for unconfined PEO melts at 80°C.

M_w	τ_R	ν_R	τ_d	ν_d
7400	1.7×10^{-7} s	9.4×10^5 Hz	2.8×10^{-6} s	5.7×10^4 Hz
17300	1.0×10^{-6} s	1.6×10^5 Hz	3.6×10^{-5} s	4.4×10^3 Hz
43200	6.0×10^{-6} s	2.7×10^4 Hz	4.3×10^{-4} s	3.7×10^2 Hz
460000	6.7×10^{-4} s	2.4×10^2 Hz	5.0×10^{-1} s	3.2×10^{-1} Hz

Results

Figure 1 shows a plot of the experimental deuteron T_1 dispersion data of PEO incorporated in a PHEMA matrix. In the frequency range above about 10^5 Hz, the data suggest a power law just as predicted in Eq. (1). An important finding is also that no dependence on the molecular mass shows up. Remarkably, this particular T_1 dispersion behavior has never been observed before with any bulk disordered melt, concentrated or semi-dilute solution system.

At low frequencies, a crossover to a dispersion plateau appears indicating a relaxation time corresponding to the transverse relaxation time T_2 in the low-frequency limit⁸⁾. The dashed line in Fig. 1 represents the experimental value measured at 9.4 T and corrected by a factor of 0.3 to obtain the limiting value for low frequencies. The small difference between the low-frequency values of the longitudinal and transverse relaxation times, T_1 and T_2 , respectively, suggests the so-called extreme narrowing case, $\omega\tau_{co} \ll 1$, where τ_{co} is the cut-off correlation time of the quadrupolar interaction in these systems. The fact that T_1 values as low as the transverse relaxation time, $T_2 \approx 3 \times 10^{-4}$ s, could be measured at the low-frequency edge also nicely proves that the plateau is no experimental artifact due to the finite resolution of the field cycle. Note that the cut-off correlation time can neither be explained with τ_d nor with

τ_R (see Tab. 2). In the present case, it rather indicates that the condition of the BWR relaxation theory⁸⁾, $T_1, T_2 \gg \tau_{co}$, starts to fail at the beginning of the plateau.

The deuteron T_1 dispersion of the same polymers, but now in the unconfined melt is plotted in Fig. 2 for comparison. The substantially different frequency and chain length dependences are obvious. The dispersion is much flatter and can be characterized in a wide range by a power law with an exponent 0.34. With the shorter chain lengths, a molecular-weight dependent low-frequency plateau appears, the onset of which is now indeed determined by a time constant that may be identified with τ_d (see Tab. 2).

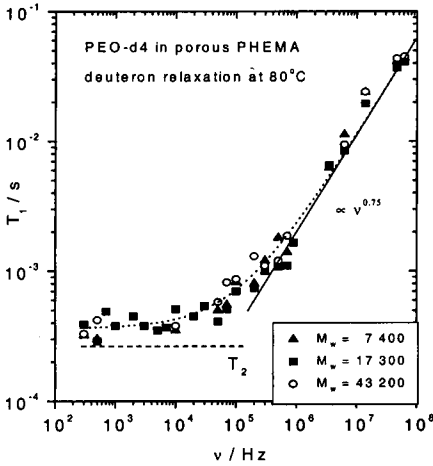


Fig. 1: Frequency dependence of the deuteron spin-lattice relaxation time of perdeuterated polyethyleneoxide (PEO-d4) in porous polyhydroxyethylmethacrylate (PHEMA) at 80 °C. Three different molecular weights were studied as indicated. The dashed horizontal line indicates the transverse relaxation time T_2 measured at 9.4 T and corrected for the low-field limit. The power law given in Eq. (1) is represented by the straight solid line in the upper frequency range.

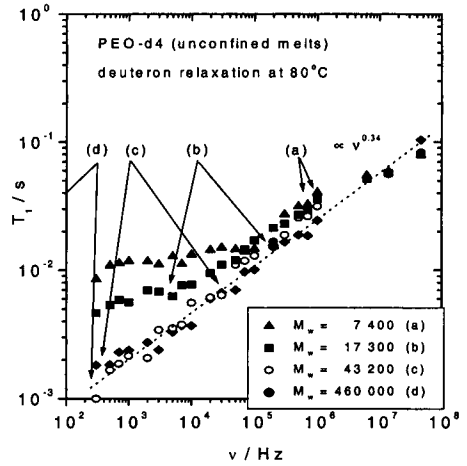


Fig. 2: Deuteron T_1 dispersion of perdeuterated polyethyleneoxide (PEO-d4) in bulk melts at 80 °C. Four different molecular weights were studied as indicated. The dotted line represents $T_1 \propto \nu^{0.34}$. The low-frequency plateaus of the two longest polymers are expected at frequencies well outside the window accessible in this study. The arrow pairs indicate the predicted ranges of limit III framed by ν_d and ν_R as estimated in Tab. 2.

The results obtained with fringe-field NMR diffusometry of linear PEO confined in the PHEMA pores are compatible with the anomalous diffusion behavior specified in Eq. 2 for $\tau_R < t < \tau_d$. The experimental data can be represented by⁹⁾

$$\langle r^2 \rangle \propto M_w^{-0.8 \pm 0.2} t^{0.6 \pm 0.1} \quad (6)$$

Conclusions

Field-cycling NMR relaxometry and fringe-field NMR diffusometry probe chain modes in the anomalous displacement regimes of entangled polymers. Linear polymer chains confined in pore channels with diameters that are comparable or smaller than the bulk random coil dimension follow the dynamic power laws predicted by the tube/reptation model in limits II and III (Tab. 1). These findings are in contrast to results obtained with melts of entangled polymers in bulk. However, the power laws observed in this case for the proton and deuteron spin-lattice relaxation dispersions can perfectly be described with the aid of a formalism linking NMR relaxation with the Renormalized Rouse theory²³⁾ and by distinguishing intra-segment and inter-segment dipolar interactions²⁴⁾.

References

1. P.G. de Gennes, *J. Chem. Phys.* **55**, 572 (1971)
2. M. Doi, S.F. Edwards, *The Theory of Polymer Dynamics*, Clarendon Press, Oxford 1986
3. H.W. Weber, R. Kimmich, *Macromolecules* **26**, 2597 (1993)
4. R. Kimmich, N. Fatkullin, H.W. Weber, S. Stapf, *J. Non-Cryst. Solids* **172-174**, 689 (1994)
5. M.E. Komlosch, P.T. Callaghan, *J. Chem. Phys.* **109**, 10053 (1998)
6. E. Fischer, R. Kimmich, N. Fatkullin, G. Yatsenko, submitted
7. E. Fischer, R. Kimmich, N. Fatkullin, *J. Chem. Phys.* **104**, 9174 (1996)
8. R. Kimmich, *NMR Tomography, Diffusometry, Relaxometry*, Springer-Verlag, Berlin 1997
9. E. Fischer, R. Kimmich, U. Beginn, M. Möller, N. Fatkullin, *Phys. Rev. E* **59**, 4079 (1999)
10. R. Kimmich, R.-O. Seitter, U. Beginn, M. Möller, N. Fatkullin, *Chem. Phys. Letters*, in press
11. W.D. Dozier, J.M. Drake, J. Klafter, *Phys. Rev. Letters* **56**, 197 (1986)
12. M.P. Bohrer, L.J. Fetters, N. Grizzuti, D.S. Pearson, M.V. Tirrell, *Macromolecules* **20**, 1827 (1987)
13. M.T. Bishop, K.H. Langley, F.E. Karasz, *Macromolecules* **22**, 1220 (1989)
14. S. Stapf, R. Kimmich, *Macromolecules* **29**, 1638 (1996)
15. M. Appel, G. Fleischer, *Europhys. Letters* **40**, 685 (1996)
16. W. Gorbatschow, M. Arndt, R. Stannarius, F. Kremer, *Europhys. Letters* **35**, 719 (1996)
17. L. Petychakis, G. Floudas, G. Fleischer, *Europhys. Letters* **40**, 685 (1997)
18. J. Kugler, E.W. Fischer, *Makromol. Chem.* **184**, 2325 (1983)
19. G.D. Smith, D.Y. Yoon, R.L. Jaffe, R.H. Colby, R. Krishnamoorti, L.J. Fetters, *Macromolecules* **29**, 3462 (1996)
20. R. Seitter, R. Kimmich, "Magnetic Resonance: Relaxometers" in *Encyclopedia of Spectroscopy and Spectrometry*, Eds: John Lindon, George Trantar, and John Holmes, Academic Press, London 1999.
21. M. Appel, G. Fleischer, *Macromolecules* **26**, 5520 (1993)
22. A.I. Maklakov, V.D. Skirda, N.F. Fatkullin, *Encyclopedia of Fluid Mechanics*, Vol. 9: *Polymer Flow Engineering*, edited by N. P. Cheremisinoff, Gulf, Houston 1990.
23. N. Fatkullin, R. Kimmich, *J. Chem. Phys.* **101**, 822 (1994)
24. R. Kimmich, N. Fatkullin, R.-O. Seitter, K. Gille, *J. Chem. Phys.* **108**, 2173 (1998)